Authors:
E. Faccioli[1], M. Vanini[2], R. Paolucci[3]

Title:

RECORD-BASED VALIDATIONS OF SITE-SPECIFIC PROBABILISTIC SEISMIC HAZARD ASSESSMENT

1) Studio Geotecnico Italiano, Via Giuseppe Ripamonti, 89, Milano, Italy (formerly at Politecnico di Milano)

2) Engineer, Via G.B. Moroni 160, 24122 Bergamo, Italy

3) Politecnico di Milano, Piazza Leonardo da Vinci 32, 20133 Milano, Italy

Corresponding author: Vanini Manuela, email: mm.vanini@gmail.com, phone:+393283825154

Abstract

Among the different approaches available to account for site specific ground response in a probabilistic seismic hazard analysis, PSHA, we have explored, with the support of instrumental data, a fully probabilistic method. In it, a probabilistic spectral site amplification function is convolved with a PSHA estimate of a spectral ordinate on rock, to obtain the corresponding spectral ordinate at the site surface. Relying on the abundant records available from the Japanese Kik-net, both at surface and downhole locations, we focused on two stations (NIGH11 and KMMH16), and derived estimations of annual mean rates of exceedance at the surface level, starting from both recorded and simulated accelerations. The simulated surface ground motions were obtained from one-dimensional, linear and non-linear wave propagation analyses, with randomized variabilities on soil stratigraphy. Two methods have been revised and checked for the computation of the convolution integral between the PSHA estimate on rock and a measure of soil amplification.

Keywords

Probabilistic seismic hazard analysis; amplification functions; uncertainties quantification; Kik-net data

This research did not receive any specific grant from funding agencies in the public, commercial, or not-for-profit sectors.

1. Introduction

In order to accurately include amplification effects in PSHA at a specific soil site, one would ideally need a single-station Ground Motion Prediction Equation (GMPE), developed from strong-motion data obtained at that site, because they would directly include the local seismic effects. If sufficient data were available, one could also directly derive, from the observations, exceedance curves for the required ground motion parameters. Only few such cases are reported and, in general, the data may not cover a range of magnitudes and distances appropriate for PSHA (e.g. Ordaz et al. 1994 [1]). In recent years, however, records by accelerometer networks in active crustal regions, e.g. the K-net and KiK-net in Japan (the NIED, National Research Institute for Earth Science and Disaster Prevention, strong-motion seismograph networks [2]), have been acquired in substantial amounts and covering broad intensity ranges.

Since such a situation is still an ideal one, in engineering practice site effects in PSHA are commonly accounted for through a "hybrid" approach, whereby the results of 1D seismic soil response analyses are superimposed on a uniform hazard spectrum at bedrock determined by probabilistic methods. In a simplified version, one may just use the site spectral amplification functions provided by seismic norms. The hybrid approach is hampered by the limitation that the quantification of the site effects does not preserve the probabilistic character of the method. At best, if the input motions used for the site response analyses are matched to the bedrock target spectrum, it may be argued that the spectrum calculated at the soil surface represents a median estimate. In addition, since the ground motion variability was already accounted for (through the GMPEs) in the PSHA leading to the bedrock spectrum, and a spread (percentile levels) associated to such spectrum was evaluated therein, the same spread could be associated to the soil spectrum (see Pecker et al., 2017 [3], for different positions on this point).

In a proper probabilistic approach, however, one must perform a convolution of PSHA results on bedrock by the site-specific amplification factor, treated as a random variable, conditioned to the exceedance of a given level of bedrock motion intensity. Although not widely known, because it appeared in a research report in Spanish, a version of the probabilistic formulation of the site amplification problem was first proposed by Faccioli and Ramírez, 1975, [4], for application at typical soft clay sites in Mexico City. For the long-duration, narrow-band earthquake motions with slowly fluctuating peak amplitude observed on the Mexico Valley clay deposits, these authors assumed that the theory of random ergodic processes could approximately be applied as regards the distribution of maxima. With this assumption, the probability that the peak acceleration on soil does not exceed a given level a_1, given the occurrence of an earthquake, was estimated as (see Udwadia and Trifunac 1973, [5], their eq. 50):

$$p(A_1 \le a_1 | \bar{a}_1^2) = F_{A_1|\bar{A}_1}(a_1 \,|\bar{a}_1) = e^{-Ne^{-\frac{a_1^2}{\bar{a}_1^2}}} = e^{-N\, e^{-\frac{a_1^2}{(A_{\bar{a}}\bar{a}_0)^2}}} \quad (1)$$

where $\bar{a}_1$ is the root mean square (rms) value of the peak amplitudes $a_1, a_2, \ldots a_N$, in a window of significant ground motion containing N positive and negative peaks. Performing 1D non-linear wave propagation analyses and assigning uncertain properties to the soil profile (and uncertain strong ground-motion duration), Faccioli and Ramírez computed a *probabilistic* amplification factor between the soft-site rms peak acceleration $\bar{a}_1$ and the corresponding value $\bar{a}_0$ at a rock site, on which seismic hazard was described in terms of exceedance curve for the peak acceleration a_0, so that the site amplification factor could be expressed as $A_{\bar{a}} = \bar{a}_1/\bar{a}_0$. $A_{\bar{a}}$was a function of $\bar{a}_0$ because of soil non-linearity effects, and was described as a random variable having as first two moments the mean and standard deviation determined from the numerical simulations. As next step, Faccioli and Ramírez performed the convolution of the conditioned distribution (1) with the density distribution (i.e. the hazard curve) of the peak rms acceleration on rock, $\bar{a}_0$, which leads to the probability distribution of the (soft) soil peak acceleration, $F_{A_1}(a_1)$, in the form:

$$F_{A_1}(a_1) = \int_0^\infty F_{A_1|\bar{A}_1}(a_1 \,|\bar{a}_1(\bar{a}_0)) f_{\bar{A}_0}(\bar{a}_0) d\bar{a}_0 \quad (2)$$

Here, $f_{\bar{A}_0}$is the density distribution of $\bar{a}_0$, and the dependence of the soil peak rms acceleration $\bar{a}_1$ on $\bar{a}_0$ enters through the amplification ratio $A_{\bar{a}}\,(\bar{a}_0)$. Faccioli and Ramírez did not use acceleration exceedance rate as hazard measure (they used the probability of exceedance in a random event, and the number of exceedances in the next T years), but such rate is easily obtained from a Poisson process assumption with known occurrence rate. Also, they used approximations for the first two moments of $A_{\bar{a}}\,(\bar{a}_0)$ derived from point-wise probability distributions to obtain a variability range for $F_{A_1}(a_1)$. A crucial point in applying the Faccioli and Ramírez method, is the selection of the most appropriate time

window of simulated or actually recorded ground motions for computing rms peak amplitudes. Sensitivity analyses discussed in a later section have shown that the window used to define the Trifunac and Brady, 1974, [6], duration is an adequate choice for calculating $\bar{a}$.

Although Faccioli and Ramírez used a different hazard measure in their original formulation, their approach is conceptually equivalent to that adopted almost 30 years later in the widely cited method of Bazzurro and Cornell (2004 a, [7], and 2004b, [8]),. This can be easily seen by comparing (2) with the Bazzurro and Cornell [8] probabilistic formulation, which reads:

$$G_Z(z) = \int_0^\infty P\left[Y \geq \frac{z}{x}|x\right] f_X(x)dx = \int_0^\infty G_{Y/X}\left(\frac{z}{x}|x\right) f_X(x)dx \quad (3)$$

where x (for rock) and z (for soil) are the random variables representing the adopted ground motion intensity, i.e. the response spectrum ordinates, and $G_Z(z)$ is the complementary distribution function, assumed to be numerically identical to the hazard. Bazzurro and Cornell [7], through a statistical study on the influence of soil profiles with uncertain properties on ground-motion intensity at the soil surface, based on nonlinear 1D wave propagation, characterized the soil effect by a frequency-dependent amplification function, $AF(f)$ (f = oscillator frequency), i.e. by the ratio of the response spectral acceleration at soil surface to that at bedrock level. Statistics of the amplification function were estimated by many nonlinear dynamic analyses of the soil column with uncertain properties, i.e., through the very same conceptual approach as in Faccioli and Ramírez. The most notable difference was the use of $AF(f)$ instead of the frequency-independent $A_{\bar{a}}$ ratio.

Until recently it has not been possible to validate ground motion hazard assessments with data covering a sufficient span of shaking intensities over an acceptable time window. However, starting from the late 1990s, ground motions of engineering significance were recorded at increasing rates at the vertical array stations of the KiK-net in Japan, which consist of a 3-component borehole seismometer placed in a bedrock formation at depth and of a surface seismometer along the same vertical, and are installed over a variety of geological site conditions, including deep and relatively soft surficial soil deposits. Although some of these stations recorded a substantial number of events across wide intensity ranges, the construction of empirical hazard curves, from such data, remains limited to annual exceedance rates above about 0.05. Nevertheless, with rock motions at depth reaching fairly strong acceleration levels (PGA up to about 0.3g), conditioned empirical amplification functions can be constructed with the many records available. Then starting from a representative/generic hazard curve on rock and using the previously recalled probabilistic approaches, one can derive a hazard curve at soil surface, through either (a) the empirical amplification functions or (b) those obtained from numerical simulations. From there, a soil/rock ratio of PSA values, at equal probabilities of exceedance PE, can be computed as a function of PE. On the other hand, an estimate of this ratio is provided by the soil/rock ratio of PSA values, at equal exceedances, directly derived from the data.

We then believe that the comparison of the latter ratio with those obtained through (a) or (b) will provide a meaningful validation of the foregoing probabilistic methods, and in this study we exploit the data recorded at two Kik-net stations to illustrate how such validation can be performed.

2. KiK-net stations data

The KiK-net stations NIGH11 and KMMH16, located as shown in Fig. 1, were selected for this study. The first lies in Central-western Honshu, in the region hit by the 2004 and 2007 Niigata earthquake sequences (both with a M_{JMA} 6.8 mainshock) , and the second in Kyushu Island, in the vicinity of the 2016 destructive Kumamoto earthquake sequence including the M_{JMA} 7.3 mainshock. NIGH11 lies in an alluvium valley, a few km wide, and KMMH16 near the edge of a coastal plane in Western Kyushu. Competent rock is found at KMMH16 at a depth of about 100 m, while at NIGH11 the soil stiffness is slowly increasing with depth, as shown in the Vs profiles of Fig. 2. Key features of the two sites, including the V_{S30} classification parameter of Eurocode 8 and the downhole (DH) instrument depths, are provided in Table 1.

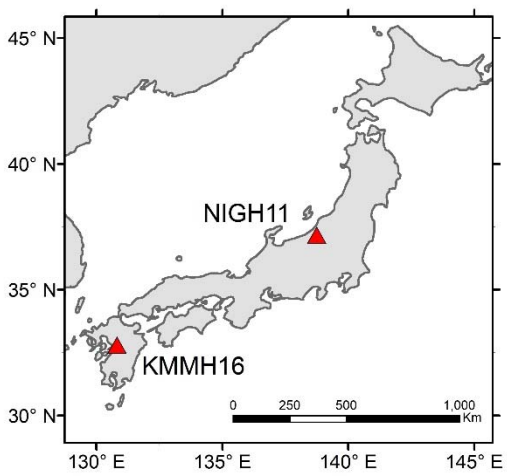

Fig. 1 Location of NIGH11 and KMMH16 KiK-net stations

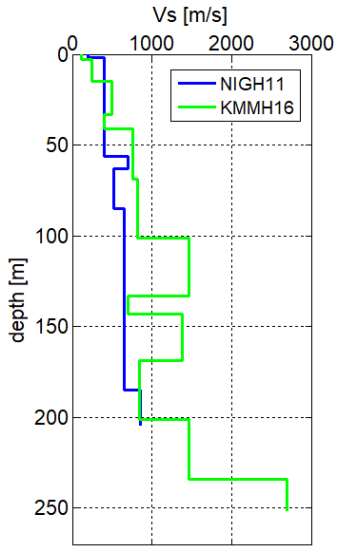

Fig. 2 *Vs* profiles at NIGH11 and KMMH16 KiK-net stations (data from NIED website)

Table 1 Summary characteristics of selected KiK-net stations

site	V_{S30} m/s	Ground category (EC8)	*Vs* at depth m/s	Depth of DH instrument m	No. of selected events
NIGH11	375	B	850	205	126
KMMH16	280	C	2700	252	113

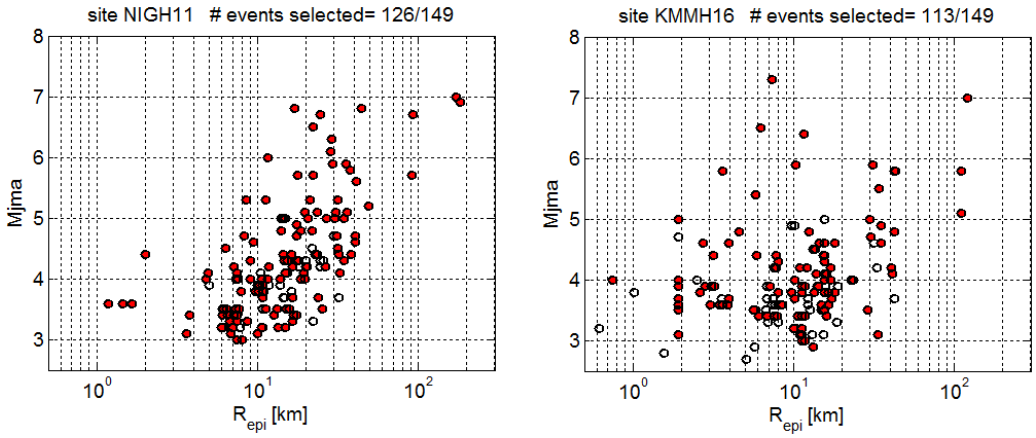

Fig. 3 Magnitude (M_{JMA}) vs. epicentral distance (R_{epi}) scatter plots of earthquakes generating the records considered at NIGH11 and KMMH16 KiK-net stations. Red circles show selected events, white circles show discarded ones

At NIGH11, within an observation period extending from 2001 to 2015, the events eligible for the analysis were selected such that: PGA ≥ 7 cm s^{-2} recorded at surface, focal depth ≤ 20 km (so as to exclude subduction events), multiple events admitted only if generating clearly separated records. The largest surface PGA value in the retained sample was 627 cm s^{-2}, and the largest DH PGA (at 205 m depth) 291 cm s^{-2}. The scatter plot in Fig. 3 shows the magnitude range of the data, from 3 to 7.0, and the distance range from, 1 to about 100 km. The two-component horizontal records from the selected events were subjected to base-line correction (average removed from whole signal), 5% tapering, zero padding, and bandpass filtering (0.05-40 Hz), in view of convolution operations performed at later stages of the analysis. Acceleration response spectra at 0.05 damping ratio were then computed for all records, and the geometric mean values among the two horizontal components have been considered.

The magnitude-distance plot for KMMH16 station is also shown in Fig. 3, and one may note that, while the intervals are about the same, the domain coverage is more uniform than for NIGH11. Since M > 6.0 events were recorded at less than 10 km distance, and Vs values as low as 110 ms^{-1} occur in the upper 10 m of the profile, significant nonlinear effects are expected to influence the site response at KMMH16 for strong shaking levels. The largest PGA at this station, recorded at ground surface, was actually 838 cm s^{-1}. The observation window extends from 2002 to 2016, with total retained events only slightly inferior to those of NIGH11. The spectral amplification function SAF = $PSA_{surface}$ / PSA_{DH} for all the retained events shows the distinct features of seismic response at the two sites, i.e. narrow-band high-frequency (T= 0.08 s) moderate amplification at NIGH11, and a wideband, much stronger amplification at KMMH16. Note the roughly constant amplification of ~ 2 across a wide period range at NIGH11.

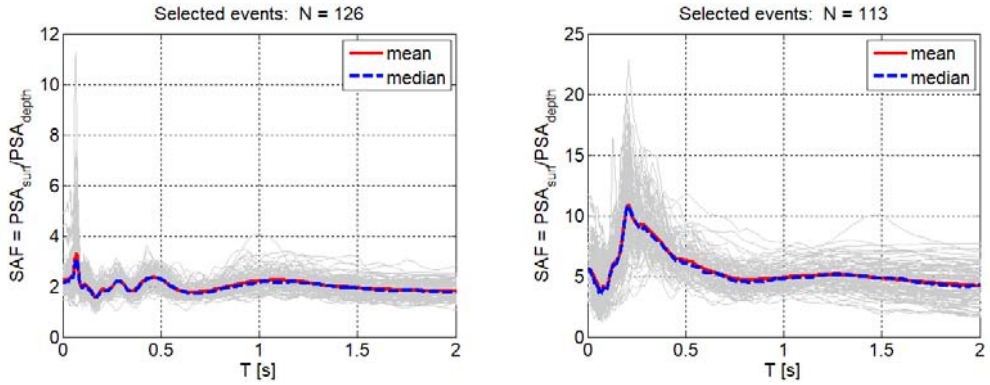

Fig. 4 Response spectral amplification at NIGH11 (*left)* and at KMMH16 (*right*)

3. Conditioned and unconditioned spectral amplification functions (SAF) at NIGH11

The evaluation of the conditioned SAF was based both on the recorded data, and on the results obtained by numerical simulations based on linear one-dimensional propagation analysis, with a frequency-dependent Q factor.

3.1 Conditioned SAF based on records

The "conditioned" SAFs (CSAFs), may be obtained by representing the spectral amplification value at a selected period vs. a measure of amplitude of ground motion at rock. We have selected for this purpose the pseudo-spectral velocity PSV=PSA·T/2π, in preference to the more commonly used pseudo-spectral acceleration PSA, because the range of variability of PSV does not change with period as significantly as for PSA, so that the same horizontal scale for different vibration periods can be used. This is shown in Fig. 5, presenting the CSAFs at NIGH11, for 0.03 s < T < 3 s, with data segregated by magnitude, vs PSV on rock (PSV^R in the figure). Conditioned SAFs show hardly any dependence on the intensity of motion at bedrock, suggesting for the station considered negligible, if any, non-linear site effects, in spite of the relatively soft soil conditions. The σ_{ln} computed from these conditioned SAFs ranges between 0.1 to 0.25, as shown in left panel of Fig. 6; no clear dependence of σ_{ln} on period is detectable.

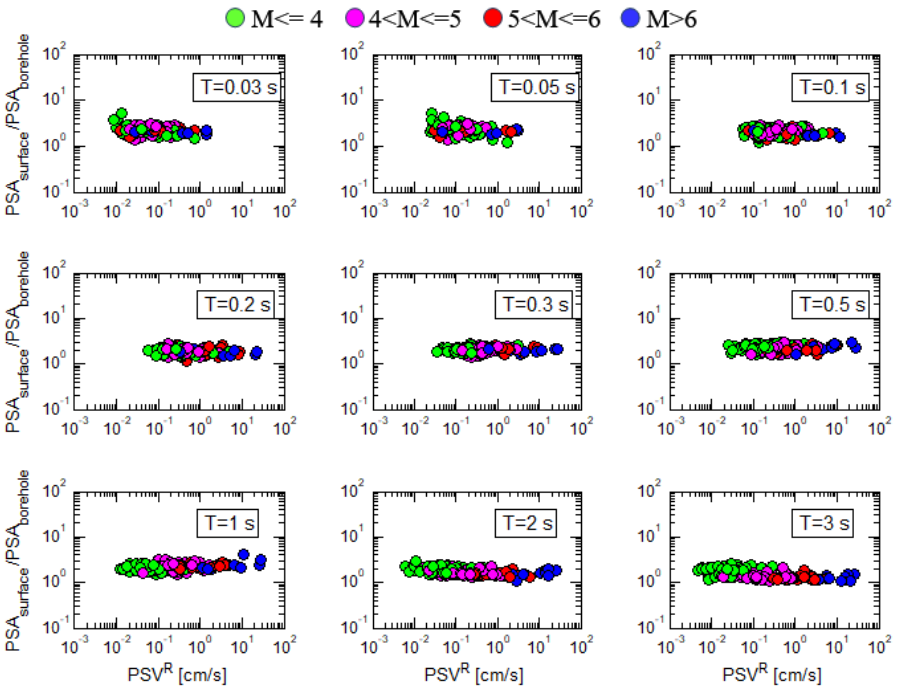

Fig. 5 Conditioned SAFs for different vibration periods, with records grouped by magnitude. Station NIGH11

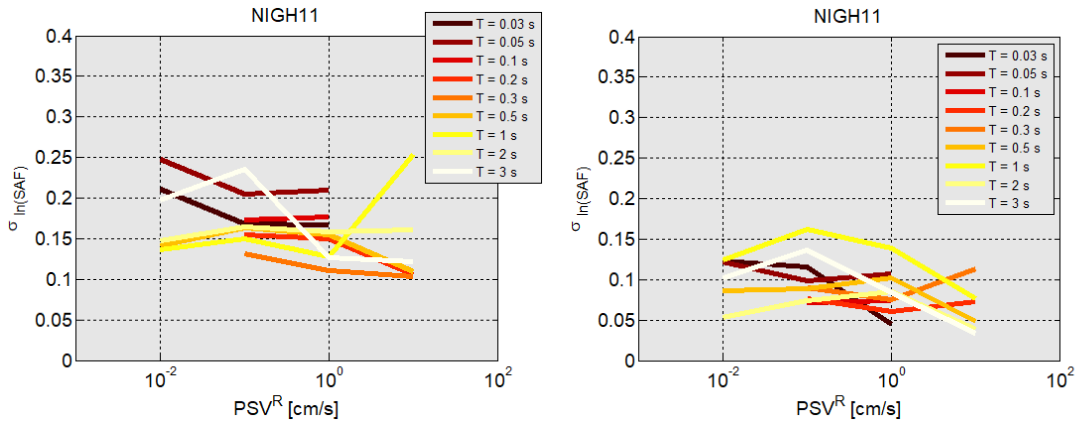

Fig. 6 Standard deviation of conditioned SAFs shown in Fig. 5 (*left*) and in subsequent Fig. 8 (*right*), for different vibration periods

3.2 Conditioned SAF based on 1D numerical simulations

Conditioned SAFs obtained from records at NIGH11, shown in Fig. 5, suggest that the soil at the site behaves linearly up to high levels of motion. This tendency has been investigated more in detail, comparing 1D analytical transfer functions with Fourier spectral ratios of surface recorded ground motion with respect to DH ones. For what concerns the quality factor Q, after substantial testing, a linear dependence with frequency has been considered, assuming $Q = Q_0 \cdot f/f_0$, where Q_0 is the adopted value (equal to $Vs/10$, where Vs is the shear wave velocity in the corresponding soil layer), assigned to the reference frequency f_0. In Fig. 7, empirical Fourier spectral ratios (mean values in red, individual values in light grey), and analytical 1D transfer functions for different values of f_0, or for constant Q, are compared. The agreement between empirical and analytical functions is good in terms of dominant frequencies, confirming the soil linear behavior; instead, the peaks of the analytical transfer functions are generally higher than the empirical ones, with a best approximation obtained when using a reference $f_0 = 20$ Hz.

Simulation of ground motions has been thus performed using a simple 1D linear visco-elastic model (corresponding to the Vs profile of NIGH11 in Fig. 2), propagating the input motions recorded at DH from depth up to the surface. The surface simulated motions have then been used to validate B&C procedure, following the same steps as for recorded motions. CSAFs, as expected, turn out to be flat (see Fig. 8), with very low standard deviations (right panel of Fig. 6).

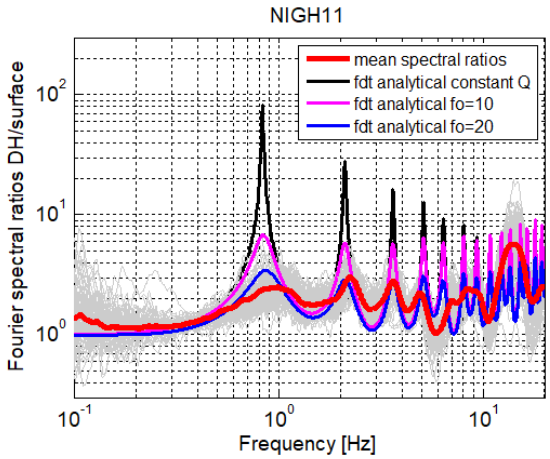

Fig. 7 Fourier spectral ratios from records (empirical transfer functions, in light grey, with mean values in red) compared with linear analytical 1D transfer functions using a constant or a frequency-proportional quality factor ($Q = Q_0 \cdot f/f_0$)

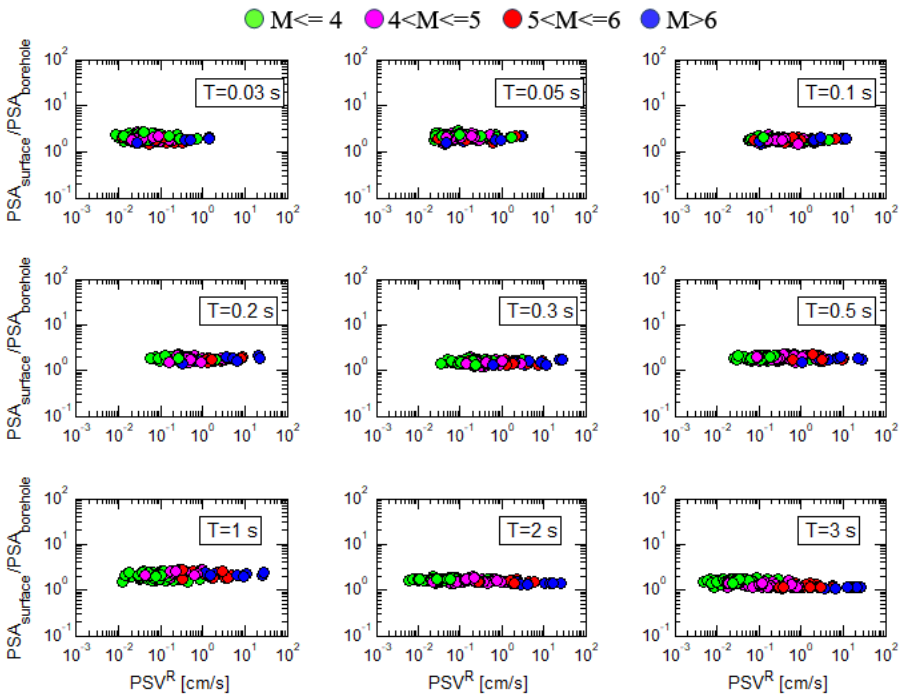

Fig. 8 Conditioned SAFs from simulated surface motions, for different vibration periods, with data segregated by magnitude values. Station NIGH11

3.3 Unconditioned SAF from seismic hazard analyses

To put the previous results in a probabilistic seismic hazard perspective, we have considered a rock hazard curve representative of a fairly high seismicity area (Fig. 9, top panel). Therefore, each spectral acceleration on rock (PSA_{rock}) is associated an annual probability of exceedance (PE), noting that, for simplicity, we denote by rock the DH Kik-net station. The corresponding spectral acceleration at soil surface (PSA_{soil}) was computed using the B&C approach, considering first the empirical conditioned SAF and, secondly, the conditioned SAF based on 1D numerical simulations. Results are shown in bottom panel of Fig. 9 in terms of PSA_{soil}/PSA_{rock} ratios, for two values of vibration period (T=0.1 s and T = 0.5 s). These ratios may be interpreted as "unconditioned" SAF, providing the spectral amplification function to be applied to the uniform hazard spectrum on rock for a given value of PE. Superimposed are the corresponding empirical PSA_{soil}/PSA_{rock} ratios, denoted by dots, computed by counting the number of exceedances, on soil and rock, respectively, of a given spectral acceleration, corresponding to a prescribed value of PE on the rock hazard curve. Although the meaning of dots and lines is different, because the empirical number of exceedances is computed on a limited time period (15 years), the large number of records makes meaningful such empirical evaluation of the site amplification function, and in reasonable agreement with the corresponding values obtained using the B&C approach. Note that although results at soil surface necessarily depend on the rock hazard curve used, the comparison of data exceedances with the B&C approach in terms of PSA_{soil}/PSA_{rock} ratios still holds, as tested using different rock hazard curve (from low up to high seismicity regions).

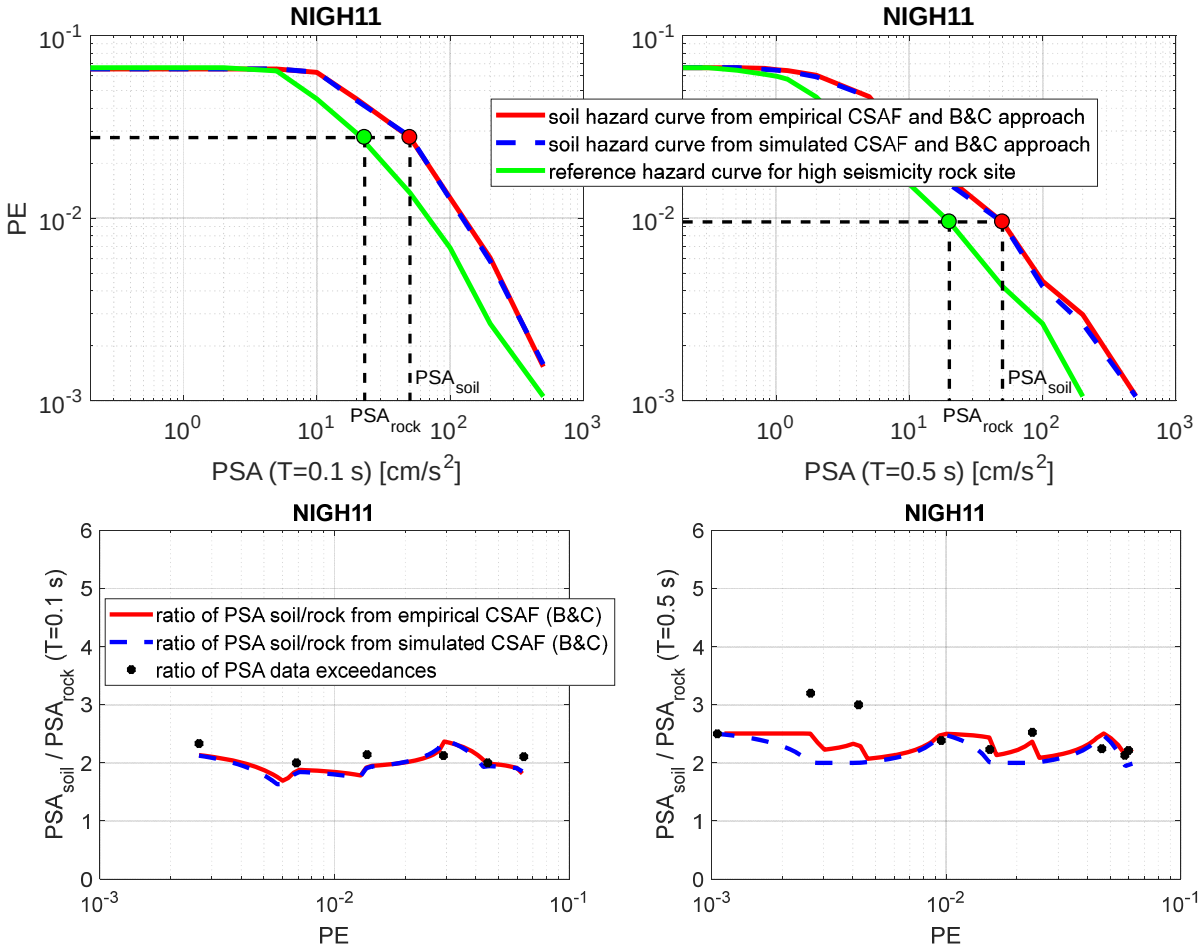

Fig. 9 Soil/rock spectral ratios as a function of PE (bottom panel). Hazard at soil surface was obtained via the B&C convolution integral approach (top panel, red and blue lines), with respect to a generic rock hazard curve (top panel, green lines). Both empirical (red) and simulated (blue) CSAF were used. Black dots show the same soil/rock ratios, computed at equal exceedance from data at surface and at DH rock location; these empirical ratios have been associated to the PE of corresponding PSA values on the rock hazard curve. Results are shown for PSA ordinates at T=0.1s (left of bottom panel) and 0.5s (right of bottom panel). Station NIGH11

4. Analysis at KMMH16

The same procedure used for station NIGH11, was also applied to the KMMH16 station. The peculiarity of the local soil response has made it necessary to adopt a different approach for simulating the surface motion: non-linear soil behavior had to be considered, as well as variability in the soil profile parameters. Evidence of probable non-linear behavior can be seen in Fig. 10, where Fourier spectral ratios from recorded set of events are plotted, segregated by surface PGA values. The program STRATA (freely available at https://github.com/arkottke/strata, Kottke et al. 2009 [9]) has been used to perform 1D non-linear propagation analyses and carefully selected soil degradation curves have been applied, as discussed further on. The variability of the input motion was introduced as well, to cast better light on the validation of the B&C procedure, when applied to sites with unknown (or not properly defined) soil characteristics.

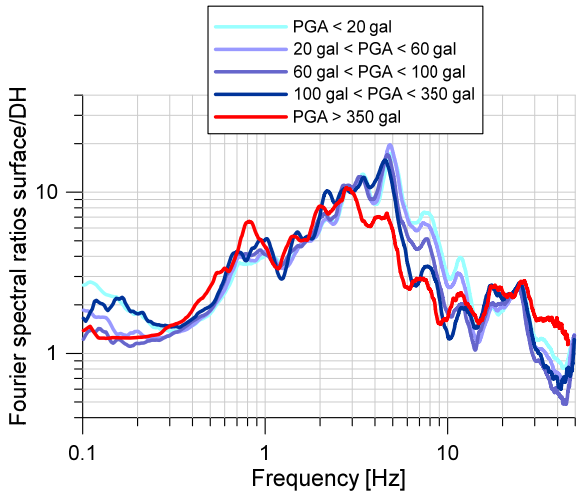

Fig. 10 Spectral amplification functions at KMMH16, segregated by PGA ranges. Note indication of clear departure from linearity starting from about 350 gal

4.1 Conditioned SAF based on records

Conditioned SAFs, shown in Fig. 11 grouped by magnitude, show a different pattern from NIGH11: amplification functions exhibit a clear dependence on the input motion intensity, especially at low structural periods, suggesting non-linear behavior. The dispersion of CSAFs values is higher than at NIGH11, but again no clear dependence of σ_{ln} on period (shown in Fig. 12) can be identified.

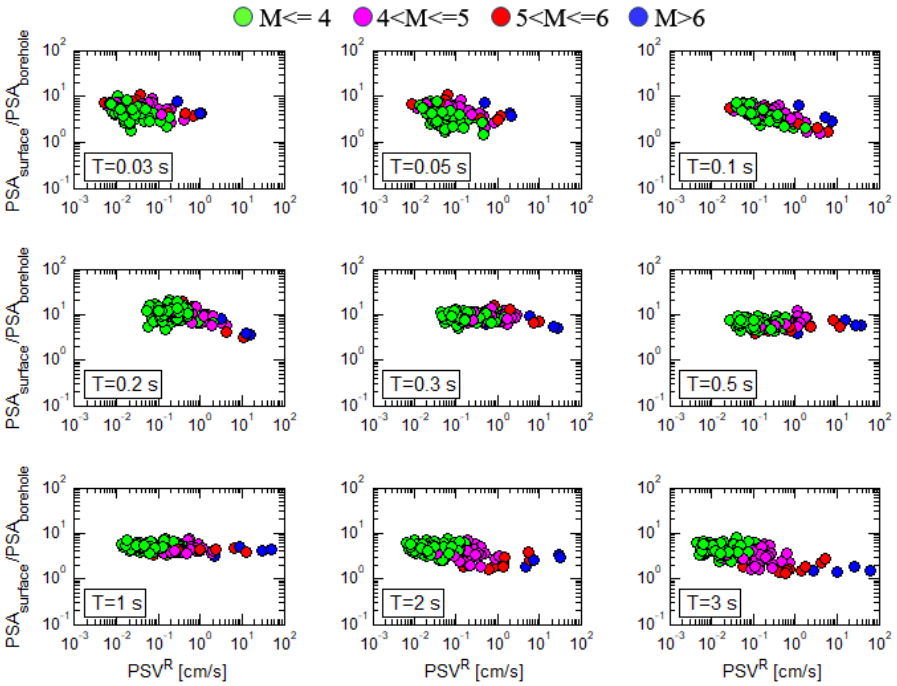

Fig. 11 Conditioned SAFs for different vibration periods, with records grouped by magnitude. Station KMMH16

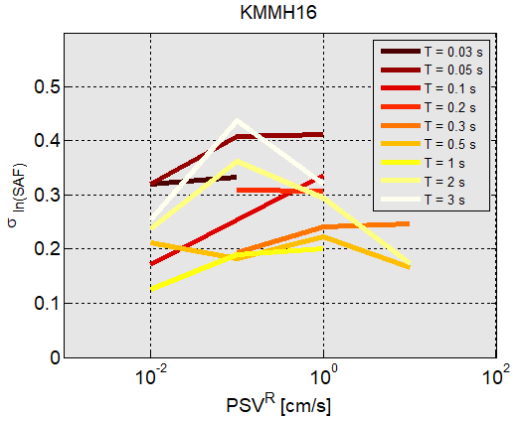

Fig. 12 Standard deviation of conditioned SAFs for the different vibration periods shown in Fig. 11

4.2 1D numerical simulations at KMMH16

The non-linear behavior suggested by CSAFs patterns has been investigated, comparing records with results from 1D linear and non-linear simulations, where DH recorded time histories were used as input motion.

The 1D linear analytical transfer function computed with the NIED velocity profile of the Kik-net station exhibits peak amplification frequencies that are poorly related with those of the empirical transfer function, i.e. Fourier spectral ratios of recorded motions (see Fig. 13). Analytical amplification levels modified according to a frequency proportional Q factor did not improve the match. In recent studies, testing the reliability of PS logging data by means of theoretical and observed HV spectral ratios (Wu at al., 2016a [10] and 2016b [11], supported by K. Irikura, written personal communication March 2017) showed that the features of the soil response at the KMMH16 site are hard to constrain even restricting the attention on weak motions alone: the use of a modified soil profile (shown in subsequent Fig. 14) proved necessary to improve fitting to the observations. For the very strong motion levels attained in the Kumamoto first strong shock (M_w 6.1, 14 April 2016) and in the mainshock (M_w 7.1, 16 April), the substantial nonlinear response effects illustrated also in Fig. 10 made the task of adjusting the velocity profile even more difficult, as discussed by Goto et al. (2017) [12]. These authors, after noting that 1D wave propagation models are more appropriate for simulating the E-W motion components, proposed different modified velocity profiles for both the weak and the strong motion ranges (where an equivalent-linear soil description was adopted based on a Ramberg – Osgood model). Nevertheless, their velocity profiles modified for the strong motion range generate response overprediction in the ~1 Hz range and underprediction in the 2-3 Hz range (where the peak spectral response occurs), quite similar to what shown herein (Fig. 15).

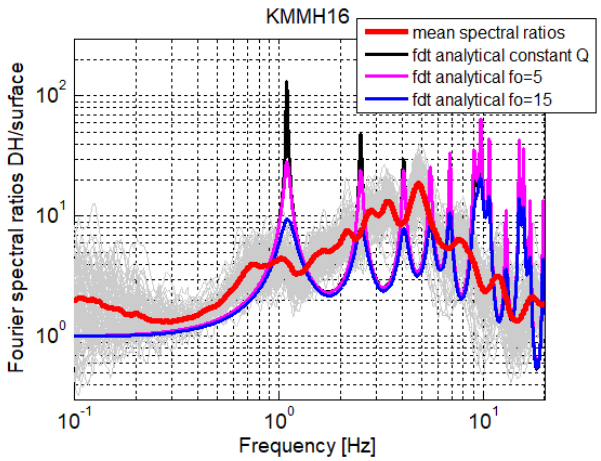

Fig. 13 Fourier spectral ratios from records (empirical transfer functions, in light grey, with mean values in red) compared with linear analytical 1D transfer functions using a constant or a frequency proportional quality factor ($Q=Q_0*f/f_0$)

Relying on the capabilities of the STRATA code (Kottke et al. 2009 [9]), and on the availability of the data simultaneously recorded at surface and DH, a new soil profile was identified for KMMH16, together with the most appropriate shear modulus (G-γ) and damping ratio (ξ-γ) degradation curves required to describe the soil non-linearity. The code performs 1D linear and equivalent-linear (SHAKE-type) response analyses using time series or random vibration theory ground motions and allows for stochastic variation of the site properties through a Monte Carlo approach, including *Vs*, layer thicknesses, depth to bedrock, and the degradation curves. Through variation of the soil properties a new soil profile was identified, shown in Fig. 14 (in blue), as the one that could minimize the differences between recorded and simulated ground motions at the surface. No changes in the layers thickness have been allowed, and only a slight variation in the *Vs* values of the deeper layers was needed to better constrain the high frequency peaks of soil response. An example of the performed simulations is given in Fig. 15, where results obtained propagating a small set of strong motions from the DH level to ground surface are shown. The model used for the analyses allowed a non-linear variation of soil properties down to a depth of 40 m; non-linearity was introduced using the Darendeli (2001), [13], degradation curves in the upper few m of clay, the standard Seed and Idriss (1970), [14], curves in the underlying sandy layers (from 9 to 15 m depth) and the Vucetic and Dobry (1991), [15], curves in the deeper clay layers. As shown in Fig. 15, the soil response at KMMH16 is not yet well described by the model adopted, especially at high frequency. However, obtaining a close constraint was out of our scope and the agreement reached has been considered good enough for the purposes of this study.

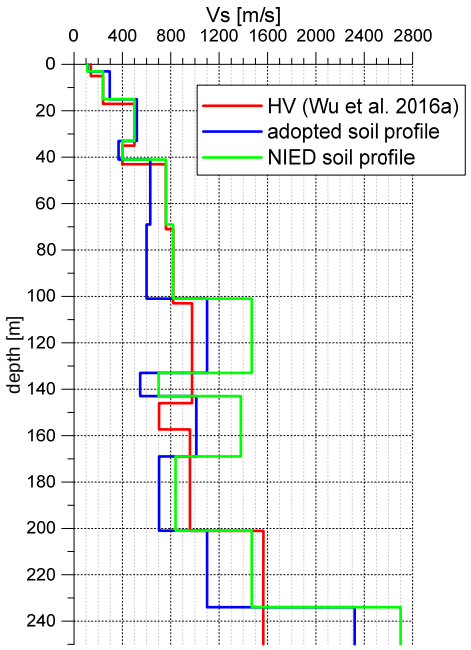

Fig. 14 *Vs* profiles at KMMH16 KiK-net station, from NIED website (green line), from recent literature studies (red line) and identified from present analyses (blue line)

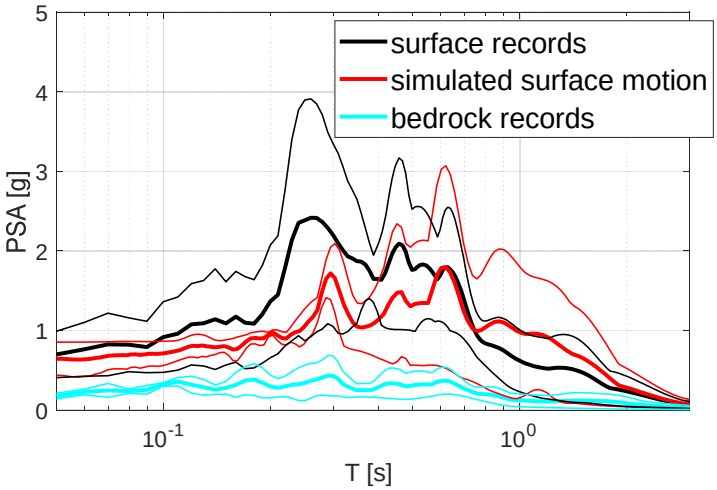

Fig. 15 Spectral accelerations simulated at the surface (red curves), using the modified velocity profile (blue curve in Fig. 14), compared with those from the corresponding records (black curves). Light blue curves show the input motion spectra, at the DH level. Mean +- 1σ are shown.

The residual uncertainties in the soil profile model have been accounted for through a variation of the soil properties, as well as of the input motion, as done in B&C 2004. Following the procedure adopted therein, two types of analyses have been conducted, i.e. a "base case" simulation test and a "randomized case" analysis. In the former, no variability of the soil column has been applied, the adopted soil profile of Fig. 14 was used and non-linear analyses were performed with the cited degradation curves, using the whole set of selected input motions (100 accelerograms). In the latter, the input motion variability has been combined with that of the soil properties, by propagation of 50 acceleration records through 100 random realizations of the soil profile. Randomized properties of *Vs* and depth of bedrock were considered log-normally distributed; the coefficient of variation was selected analyzing the uncertainties of similar soil profiles in the Po Plain, Northern Italy, region (with COV *Vs* varying between 0.15, at ground surface, and 0.35 at bedrock level; COV *Vs* at bedrock level was chosen as 0.13, see Garofalo et al. 2016 [16]). Variability of G/G_{max} and damping curves was assigned relying on the built-in standard deviation model and correlation coefficients of STRATA.

Input motions were selected from the Cauzzi & Faccioli (2008), [17], GMPE database, with the following criteria:

1. Recording sites on ground category A and B subsoil with $V_{S30} > 500$ m/s
2. M_w between 4.5 and 7.6
3. $R_{hypo} < 100$ km
4. PGA ≥10 gal.

A set of one hundred records was selected for each component of motion (100 for EW components, and 100 for NS components); from this set, a total of 100 records were used in the amplification study (base case), choosing 1 horizontal component per record, at random. 50 of these records where used for the randomized case propagation analyses. The M_w and R_{hypo} parameters of the selected data have a reasonably even distribution in their selection intervals, see [17]. The variability of the input motions is comparable to that of the B&C analyses in the low period range, while slightly higher at low frequency.

The set of input motions was applied on the outcropping stiff ground layer with *Vs* = 630 m/s, as shown in the diagram of Fig. 16. Each input motion was propagated down to the borehole level and then up to the ground surface. Pseudo spectral accelerations computed at the surface and at the DH level were used to estimate the numerical conditioned SAFs (= $PSA_{surface}$ / $PSA_{bedrock}$).

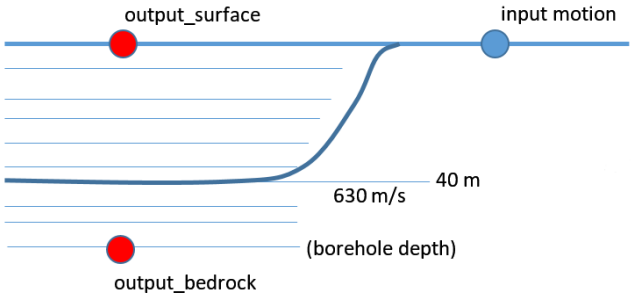

Fig. 16 Diagram of numerical simulations performed for KMMH16 station

4.3 Conditioned SAF from numerical simulations

Fig. 17 shows the simulated spectral amplification functions from the base case (*left*) and randomized case (*right*) respectively. Due to the high number of simulations (50 accelerograms times 100 profiles), details of local peak amplifications are less perceptible in randomized case results, as expected, though amplification levels and related dispersions are comparable. The mean SAF computed from records are shown for comparison in the same plots. SAF from events with M >= 4.5 have been computed separately, consistently with the input motion levels used in simulations. Note that the estimated amplifications (red lines in figures) are much smaller than observed ones (blue lines), particularly around the peak value of 0.2-0.3 s, confirming that the adopted soil model, as already discussed, is not yet satisfactory enough at those frequencies. Dispersion values are comparable to those of B&C 2004a [8] (see figures 5 and 15 therein), although variability does not significantly increase with frequency as for B&C.

Fig. 18 shows details of SAF obtained from base case simulations, grouped by PGA of input motions: non linearity of response clearly shows for records with PGA exceeding 0.4 g, when peak amplifications move towards lower frequencies (about 1 Hz).

CSAFs from simulations are shown in Fig. 19, for base case (*left*) and randomized case (*right*) respectively, while related standard deviations are in Fig. 20. Note that CSAFs are strongly magnitude dependent, the non-linearity in soil response being particularly evident at low period (0.1 s), as for observed CSAFs, when data were segregated by the same magnitude ranges (not shown). As the period decreases, the non-linear effect is more evident even at low levels of input motions. The average dispersion of CSAFs increases, as expected, with the number of simulations, and tends to lower values at longer period (3 s), opposite to observations (Fig. 12). Standard deviation patterns of CSAFs were noted to be strongly influenced by the characteristics of the soil profile (not shown), although average values do not change significantly. Standard deviations of randomized case increase as they include the variability of the input motion (present in base case) as well as the variability of the randomized soil profile.

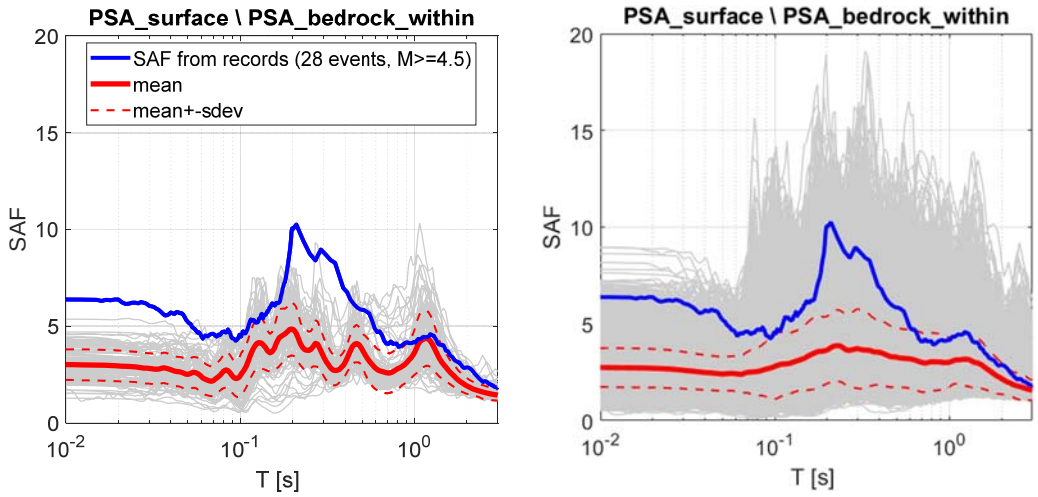

Fig. 17 Amplification functions with respect to bedrock within motion. Simulated base case (*left*) and randomized case (*right*) are shown in red (mean +- sdev). SAF from records are shown in light blue, for M>=4.5 events.

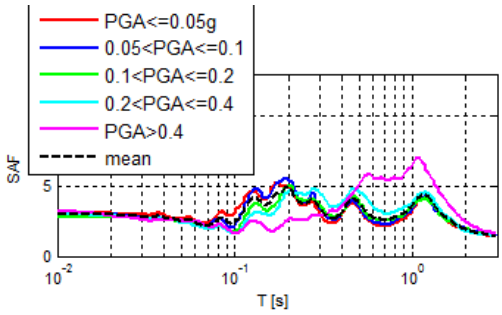

Fig. 18 Simulated SAFs with respect to bedrock "within" motion, segregated by input PGA. Base case analyses.

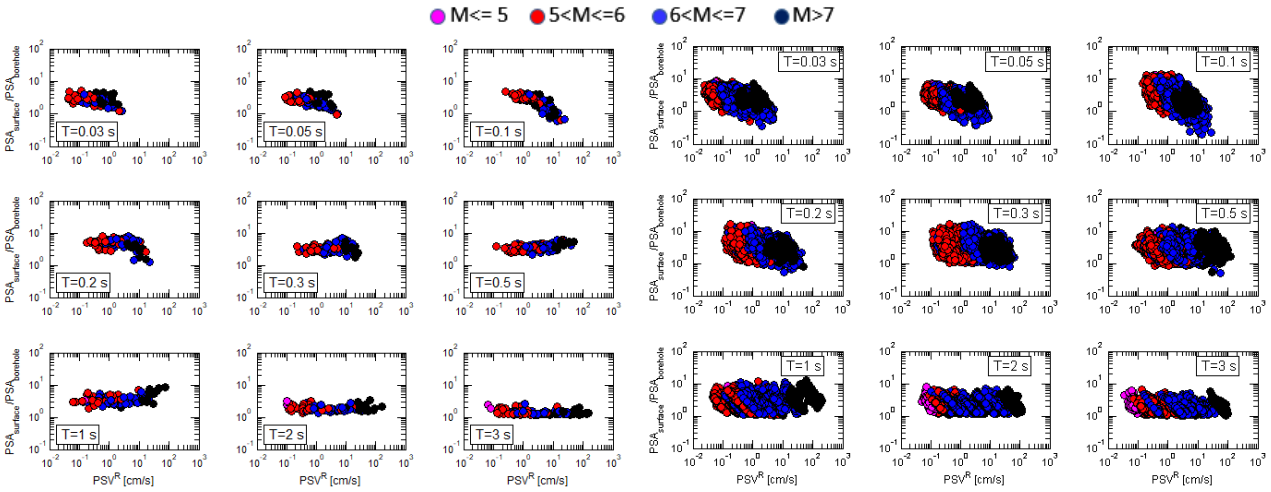

Fig. 19 CSAFs from simulations. Base case (*left*) and randomized case (*right*).

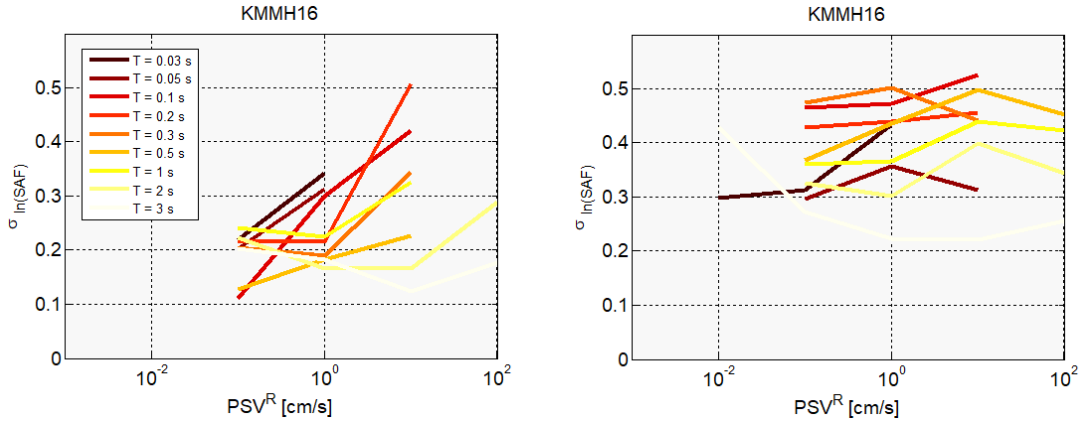

Fig. 20 Standard deviations of CSAFs for the periods shown in Fig. 19. Base case (*left*) and randomized case (*right*).

4.4 Unconditioned SAF from seismic hazard analyses

Similarly to NIGH11, starting from a representative rock-hazard curve (at DH location), the soil-hazard curve has been evaluated with the B&C convolution integral (3), considering the CSAF based both on records and on 1D numerical simulations. Results for $T = 0.1$ s and 0.5 s are shown in Fig. 21 in terms of soil/rock spectral ratios at given PE values, for both base case (brown curves) and randomized case (blue curves) simulations. A very good agreement is evident between empirical CSAF results (red curves) and observed soil/rock spectral ratios (black dots) at all exceedance levels. Similar results have been found for all other structural period, thus validating the applied procedure.

Note the high amplification levels, with respect to NIGH11 consistently with SAF of Fig. 4, 11 and 12. (Actual values of amplification have a relative importance, as they are related to a reference rock that is in these analyses at DH position, for SAF and for computed hazard curves).

Discrepancies of simulated motions with respect to observed soil/rock spectral ratios (black dots in figure) for a given PE increase near the periods where the simulated CSAFs cannot account for observed soil amplifications, e.g. for T=0.2-0.5 s, as shown in Fig. 17. Unexpectedly, differences between the base and the randomized case simulations are small, although for latter simulations the difference with respect to observed amplifications tend to increase, e.g. at T = 0.2 s or 1 s (not shown), probably due to peculiar SAF patterns: the mean amplification values of randomized case show a decrease at these periods of about 25% and 20 % respectively with respect to base case (see Fig. 17). Despite an increase in the standard deviation σ_{lnSAF} of the randomized case, this parameter is found to have less influence on final results than the absolute values of the CSAF (tested, but not shown).

As observed and tested, the accuracy of the method depends on how closely the local site amplification features are accounted for by the soil profile model used. In particular, results will deteriorate where the site resonance frequencies will be missed or poorly predicted by the adopted SAF.

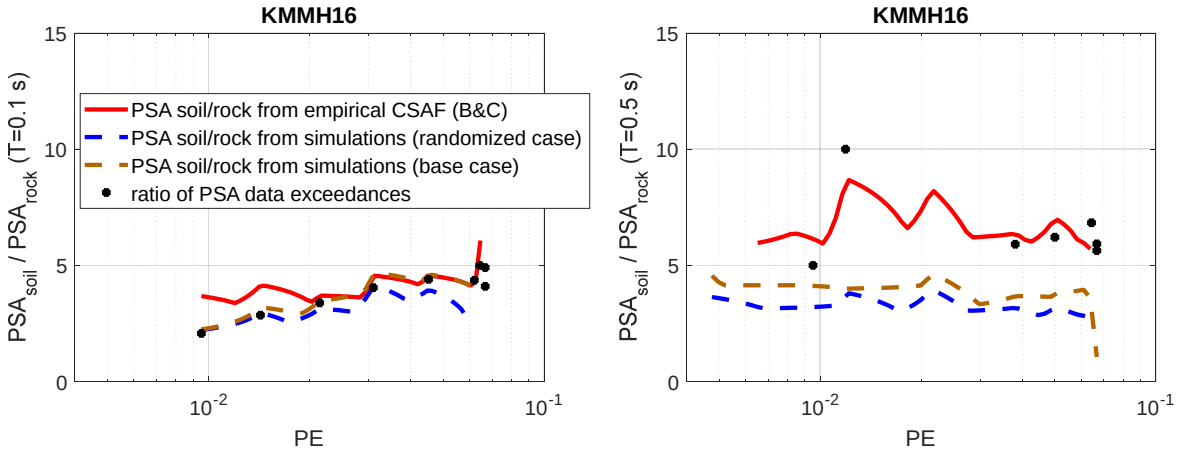

Fig. 21 Soil/rock spectral ratio values as a function of PE for vibration periods of 0.1 and 0.5 s, obtained via the B&C convolution integral approach applied to observed (red line) and simulated surface motions (blue line, for randomized case simulations, brown line, for base case simulations), compared with the observed soil/rock spectral ratio at selected exceedance values (black dots)

5. Validation analysis of the Faccioli and Ramirez (1975) method at KMMH16

Also a validation of the Faccioli and Ramirez (F&R) approach, described in the Introduction, has been performed using the station KMMH16 dataset, selected on the basis of magnitude and peak value ranges, in order to test the viability of the underlying assumptions.

The starting point, as previously pointed out, is the computation of $\bar{a}$, the root mean square of the peak values of recorded time histories, both at surface and DH level, according to the well-known definition:

$$\bar{a} = \sqrt{\frac{1}{N}\sum_{i=1}^{N} a_i^{\,2}} \qquad (4)$$

where a_i are the N peak amplitudes of the record, both positive and negative, in the window of significant ground motion duration. This duration has a strong influence on the computation of $\bar{a}$; in this work, after a series of sensitivity analyses, the significant duration defined by [6] has been chosen. Fig. 22 shows the calculation of $\bar{a}$ for two events with different magnitude values, i.e. M_w 3.4 and M_w 5.8. Plots display (with red asterisks) the peak values actually considered in the significant duration intervals. Note that the value of $\bar{a}$ is only weakly dependent on magnitude, especially at DH level, justifying the use of both low and higher magnitude motions in calculations. The observed number N of positive and negative peaks, used in eq. (4), is distributed with magnitude as shown in Fig. 23; its median values of N are about

90 and 70 for DH and surface records respectively. A flat value of 100 has been actually introduced in final calculations using eq. (1), after extensive testing.

Ratios of peak ground acceleration, PGA, over $\bar{a}$ have also been computed, to detect any significant dependence on magnitude or epicentral distance. The PGA/ $\bar{a}$ ratios do not seem to depend on magnitude, or on distance (not shown), having predominant values of about 4 at DH level, and lower than 2, at the surface, with reduced dispersion. Only few events exhibit higher ratios, mainly due to local recorded spikes, not related to magnitude. The influence of these events on final results has been tested in computations, and was found to be quite modest.

The core of the F&R method, as illustrated in equations (1) and (2), is the computation of the ratios of $\bar{a}$ values, surface with respect to DH, conditioned to the DH $\bar{a}$. These ratios, shown in Fig. 24, clearly display non-linearity features that have to be adequately considered in the convolution integrals for the prediction of $\bar{a}$ on soil. In Fig. 24, the mean conditioned ratio actually used in computations is shown. The standard deviation of this conditioned amplification function, denoted as $A_{\bar{a}} = \bar{a}_1/\bar{a}_0$ in (1), is not directly used in the integral in (2), as in B&C method, but it may be introduced through mean ± 1σ values for $A_{\bar{a}}$ (shown in the figure) to take the uncertainty of estimation into account.

The implementation of the approach requires the computation of the integral of (2), where the density distribution of $\bar{a}_0$ has to be introduced. As in the B&C approach, this distribution was obtained by differentiating a reference rock-hazard curve for $\bar{a}_0$. Conditioned amplification functions have been derived using different sets of records, to test the influence of lower magnitude events, as well as of outlier PGA/$\bar{a}$ values. The final results of the application of the F&R approach are shown in Fig. 25, in terms of spectral soil/rock ratios at give PE values (computed as explained in previous sections), comparing predicted curves (in blue) with those obtained from records (black dots), and with results from the B&C method as well (red lines). Only results obtained from all records of KMMH16 database are shown in Fig. 25. As evident, the F&R approach tends to slightly underestimate the surface amplification level, and more so for PE > $2x10^{-2}$, while the B&C approach, although more accurate for low annual rates, tends to be over-conservative for low probabilities of exceedance. When used for validation against recorded data, the accuracy of these methods, especially the F&R one, strongly depends on the robustness of the available data sample on both bedrock and soil: the more records is included (in a range of engineering interest), the more accurate the estimated convolution will be (not shown). The F&R results depend as well on the number of the *N* of positive and negative peaks considered in the cumulative distribution (1); as discussed, a flat value *N*=100 seemed as a reasonable approximation, coherent with observations. Also to be noted is the potential usefulness of having a measure of the variability band attached to the F&R method, deriving in this case only on the variability of the $A_{\bar{a}}$ ratios from the data. Using the mean + 1σ level for $A_{\bar{a}}$ leads the predicted amplification almost to coincide with the observed one (at least for PE>10^{-2}).

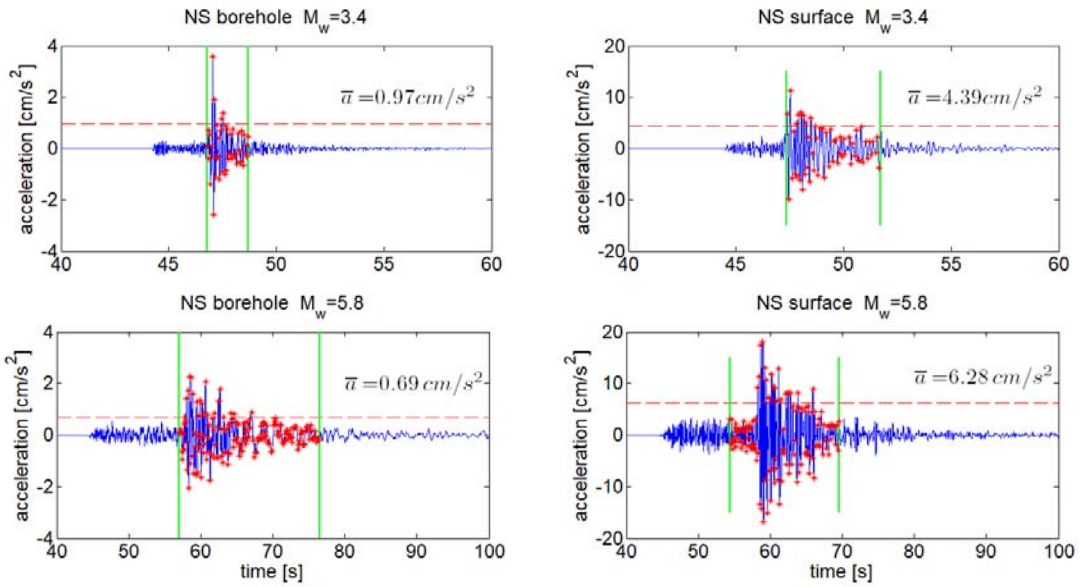

Fig. 22 Examples of calculation of peak rms acceleration $\bar{a}$ on waveforms of two events (M_w=3.4, *top*, M_w=5.8, *bottom*). Green lines delimit the Trifunac&Brady (1974), [6], duration window, horizontal red dashed line shows $\bar{a}$ value, red asterisks show positive and negative peaks entering the computation.

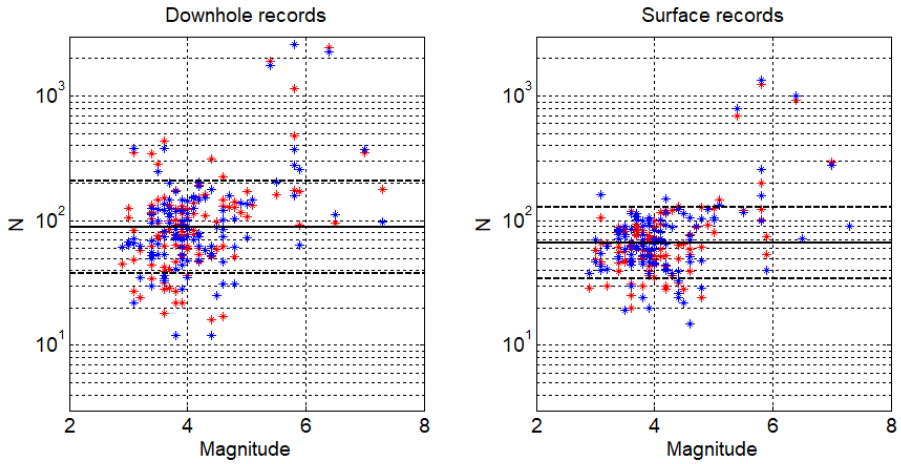

Fig. 23 Number *N* of positive and negative peaks from records (red asterisks of Fig. 22)

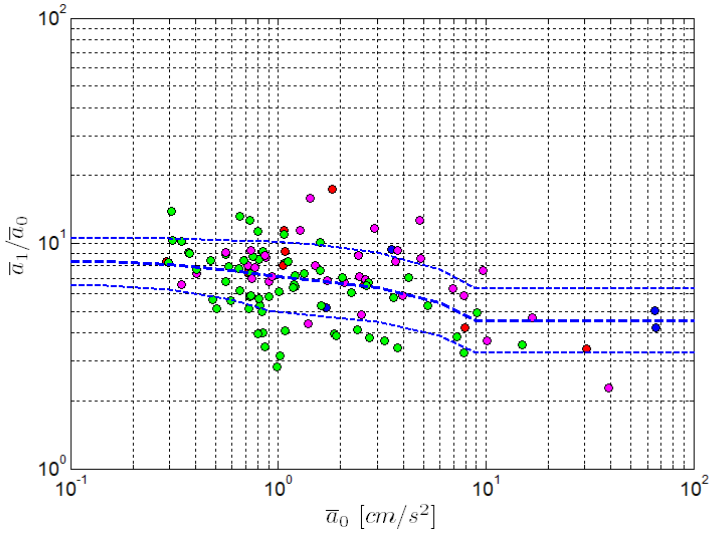

Fig. 24 Conditioned rms acceleration ratios versus DH rms acceleration, from data, segregated by magnitude ranges. Blue line show mean interpolated ratio actually used in the convolution integral (2), blue dashed lines show mean +- st.dev.

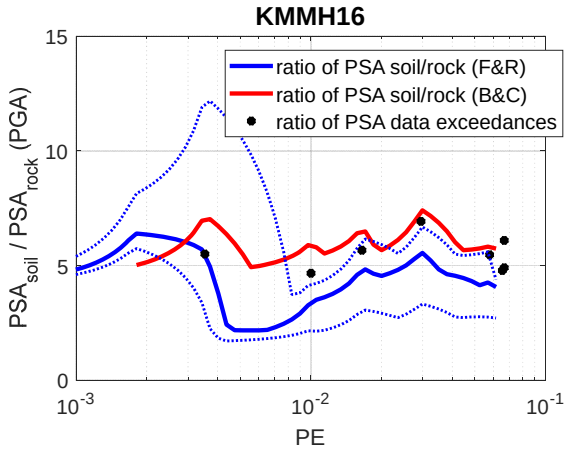

Fig. 25 Ratio of soil/rock spectral values at given PE, from hazard curves obtained at soil surface, via the F&R approach (blue line) and the B&C approach (red line), with respect to a generic rock hazard curve. The soil/rock spectral ratio computed from data is shown for comparison as well (black dots). KMMH16 station

6. Concluding remarks

A sizable amount of accelerometer records available for the two vertical array stations NIGH11 and KMMH16 of the Japanese KiK-net, generated from events in the $3 < M_{JMA} < 7$ and $1 < R_{epi} < 100$ km ranges over a time span of about 15 years, has allowed us to test the prediction capability of two methods for site-specific PSHA. These are the little known precursor method of Faccioli and Ramírez (1975), [4], and the widely known one of Bazzurro and Cornell ([8] and [9]). Both start from a hazard curve *on rock* for a ground motion parameter, and yield as result the corresponding hazard curve at *soil surface*, obtained through a convolution integral that hinges around a conditioned spectral amplification function. Such function is expected in both methods to be calculated from 1D wave propagation analyses through a soil stiffness profile with uncertain properties, using as excitation an appropriate set (that can be large) of acceleration time histories. While the Bazzurro and Cornell approach holds for a generic response spectrum ordinate, that of Faccioli and Ramírez, based on RV theory, was originally restricted to the prediction of PGA, although it can be easily extended to any spectral ordinate. The applicability of both methods was tested first through the exclusive use of the records recorded down-hole (DH) and at the ground surface. The surface exceedance rates were obtained from direct application of the analytical expressions (1) - (2) and (3), for the two methods respectively, using the conditioned

spectral (or rms peak acceleration) amplification function also derived from the observed spectral ratios. A counting procedure was applied to the surface and DH spectra to obtain exceedance levels to be compared with simulations, in terms of PSA spectral ratios at given PE. The closeness of the simulated soil/rock spectral ratios to those obtained from direct counting on records has been regarded as the primary indicator of the performance of the method. In this kind of testing the data of both NIGH11 and KMMH16 were used for the Bazzurro and Cornell method, but only those of KMMH16 for the Faccioli and Ramírez method. On the other hand, the testing of the Bazzurro and Cornell method, based on propagation of many acceleration signals through a large number of randomized soil profiles was conducted in full only for the KMMH16 site.

Although the velocity profiles at the two stations differ by less than 100 ms^{-1} in terms of V_{S30}, with KMMH16 in the upper range of Eurocode 8 category C sites (CEN 2003) and NIGH11 just above the C/B boundary, the two sites significantly differ in amplification features. This is shown by the response spectral amplification functions in Fig. 4, in terms of mean values, and in Fig. 5 and Fig. 11, conditioned to the peak values of downhole bedrock motion. In their conditioned form, spectral amplification functions at NIGH11 are almost constant as a function of the amplitude of input motion, corresponding to an essentially linear response, while at KMMH16 a decreasing trend for large values of input motion is apparent, below about 0.2 – 0.3 s, thus suggesting a non-linear response.

For NIGH11, 1D linear visco-elastic wave propagation through the reference soil profile (Fig. 2) allowed us to obtain results in very good agreement with those based on records (Fig. 9). For this purpose, a frequency-proportional Q-factor was required, instead of the more common frequency-independent assumption, to improve the accuracy of prediction of peak amplification values. Furthermore, due to the satisfactory results, no effect of the randomization of the soil profile was explored.

For the KMMH16 records, the analysis yielded a different picture, due to the amplification levels driven by the stronger impedance contrasts (notably at about 15 m and 100 m depth) and the soft upper portion of the profile at this site. As in the case of NIGH11 (Fig. 9), the results of the Bazzurro and Cornell approach based only on the site records matched closely the exceedance rates from the observations (Fig. 21). In spite of its good performance when using records, the validation using 1D numerical simulations with all the ingredients of the Bazzurro and Cornell approach, i.e., a large database of external acceleration inputs and the introduction of sizable variability in soil properties (50 acceleration records propagated in this case through 100 random realizations of the soil profile) proved only partially successful at KMMH16. Results underpredicted the observed amplifications, more notably for vibration periods from 0.2 s to 0.5s; only the zero-period spectral ordinate (PGA) was slightly overpredicted. Inaccuracy of the published Vs profile (measured by NIED with P-S wave logging technique) is believed to be the most likely cause of the discrepancy (pictured notably in the graphs of Fig. 21, for T=0.5s) despite the fact that these results were obtained using as a point of departure the "adopted soil profile" of Fig. 14, in which corrections to the NIED profile were introduced to improve the agreement of dominant frequencies in the surface spectra. The randomization process of the soil profile led to an increased underprediction of amplification levels, consistently with the smoothing of the related SAF values, and notwithstanding the increase in the standard deviation of the CSAF. The lesson from this case is that, even when using a rigorous approach such as the Bazzurro and Cornell method, the reliability of the site-specific amplification levels obtained (and so of the related surface hazard curve) critically depends on the quality of the soil profile model available and that if, in particular, this leads to poorly estimating the site dominant frequencies, the calculated hazard curves on soil will be unreliable, precisely where their influence on design could be more critical.

Finally, the Faccioli and Ramírez precursor method of 1975 has been successfully applied to estimating PGA hazard curves for the first time outside the context for which it had been specifically devised, i.e. the probabilistic seismic response of the soft clay deposits in the Mexico valley (where the RV approach tends to work well). The critical element in this application was found to be the selection of the significant ground motion duration over which the rms peak acceleration level is evaluated: the Trifunac and Brady definition of duration was found to be practical, although it may in some cases lead to underestimating the rms acceleration levels of interest. This approach seems to have a tendency opposite to that of Bazzurro and Cornell (in the case of PGA), since it tends to slightly underestimate the

amplification levels at ground surface. On the whole, however, it seems that when dealing with the estimation of PGA hazard curves the combined use of both methods would tend to bracket the observed amplification levels.

Acknowledgments

We are indebted to one reviewer for pointing out to us a flaw that negatively affected the first version of the manuscript.

7. References

[1] Ordaz M, SK Singh, A Arciniega (1994). Bayesian attenuation regressions: an application to Mexico City, Geophys. J. Int., 177, 335-344.

[2] http://www.kyoshin.bosai.go.jp/. Accessed July 2017.

[3] Pecker A, Faccioli E, Gurpinar A, Martin C, Renault P (2017) An Overview of the SIGMA Research Project - A European Approach to Seismic Hazard Analysis. Geotechnical, Geological and Earthquake Engineering, Springer International Publishing AG, ISBN 978-3-319-58153-8

[4] Faccioli E, Ramírez J (1975) Respuestas sísmicas máximas probables en las arcillas de la Ciudad de México. Informe 359, Instituto de Ingeniería, Universidad Nacional Autónoma de México, Mexico City

[5] Udwadia, F. E. and Trifunac, M. D. (1973) The Fourier transform, response spectra and their relationship through the statistics of oscillatore responbse, Report No. EERL 73-01, Earthquake Engineering Research Laboratory, California Institute of Technology, Pasadena California

[6] Trifunac M, Brady AG (1974) A study on duration of strong earthquake ground motion. B Seismol Soc Am 65(3): 581-626

[7] Bazzurro P, Cornell CA (2004a) Ground-motion amplification in nonlinear soil sites with uncertain properties. B Seismol Soc Am, 94(6): 2090-2109

[8] Bazzurro P, Cornell CA (2004b) Nonlinear soil-site effects in probabilistic seismic-hazard analysis. B Seismol Soc Am, 94(6): 2110-2123

[9] Kottke AR, Rathje EM (2009). Technical Manual for Strata. PEER Report 2008/10, University of California, Berkeley, February 2009

[10] Wu H, Susumu K, Kazuaki M, Kojiro I (2016a). Site amplification at strong-motion stations in the Kumamoto prefecture and identification of underground velocity structures at Mashiki. Japan Geoscience Union Meeting 2016, May 22nd-26th, Makuhari Messe. MIS34-P79

[11] Wu H, Masaki K, Kojir I (2016b). An alternative method to identify underground velocity structures from microtremor H/V spectral ratio. 5th IASPEI/IAEE Int Symp: Effects of Surface Geology on Seismic Motion, August 15-17, 2016

[12] Goto H, H Yoshiya, Y Masayuki, Y Nozomu (2017). Nonlinear Site Response at KiK-net KMMH16 (Mashiki) and Heavily Damaged Sites during the 2016 Mw 7.1 Kumamoto Earthquake, Japan, B Seismol Soc Am 20 (20), doi: 10.1785/0120160312

[13] Darendeli MB (2001) Development of a new family of normalized modulus reduction and material damping curves. PhD dissertation, Univ. of Texas at Austin

[14] Seed HB, Idriss IM (1970) Soil Moduli and Damping Factors for Dynamic Response Analysis, Report No. UCB/EERC-70/10, Earthquake Engineering Research Center, University of California, Berkeley, December, 48 p. (as cited in the EERA Manual, Bardet et al., 2000)

[15] Vucetic M, Dobry R (1991). Effect of soil plasticity on cyclic response. Journal of the geotechnical Engineering Division, ASCE, 17(1): 89-107

[16] Garofalo F, Foti S, Hollender F, Bard PY, Cornou C, Cox BR, Dechamp A, Ohrnberger M, Perron V, Sicilia D, Teague D, Vergniault C (2016) InterPACIFIC project: comparison of invasive and non-invasive methods for seismic

site characterization, Part II: Inter-comparison between surface-wave and borehole methods. Soil Dyn Earthq Eng 82:241–254

[17] Cauzzi C, Faccioli E (2008). Broadband (0.05 to 20 s) prediction of displacement response spectra based on worldwide digital records, J Seismol, 12:453–475